THE STRUCTURAL MODELLING OF ROTATING BLADES

A. Rosen and O. Rand
Department of Aeronautical Engineering
Technion - Israel Institute of Technology
Haifa 32000, Israel

Abstract

The paper presents a structural model of rotating blades. The model can deal with straight blades and curved blades having any planar curvature. In addition any distribution of the structural properties along the blade and any distribution of loads along the blade can be dealt with. The model itself is nonlinear and satisfies the conditions of small strains and moderate elastic rotations. Special effort has been devoted in order to obtain a consistent model with a minimum number of simplifying assumptions. Besides dealing with the nonlinear homogeneous set of boundary conditions, there is also a capability of analysing cases of elastic restraints at the root, which are very common in practical cases of blades. The solution is obtained by using Galerkin method. Two techniques are used in order to calculate the cross-sectional resultant forces and moments along the blade: the first method is based on differentiation of the expressions of the displacements along the blade, while the second method is based on integration of loads along the blade. In order to present the capabilities of the model numerical examples are presented and discussed.

I. Introduction

Rotating blades appear in many aeronautical applications. These applications include: propeller blades, helicopter blades, jet engine blades and others. The analysis of these rotating blades is a very complicated task where different aspects are still not fully understood and deserve further thorough investigation in the future. The reason for the complexity of the analysis of rotating blades is the fact that this behavior is the result of the coupled influence of: structural, inertial and aerodynamic contributions. Each of these contributions is very complicated by itself and the interaction between the three makes the problem even more complicated. In analysing the behavior of blades it is important that each of the contributions will be described by a model whose accuracy is identical to the accuracy of the other two contributions. If this is not the case than an unbalanced model is obtained. The results of such models are questionable.

The purpose of the present paper is to present a consistent model of the structural contributions to the blade behavior. This model is restricted to the case where, from a structural point of view, the blade can be looked upon as a slender rod. Cases of low aspect-ratio blades, which should be modeled as shell-like structures, are not considered here.

During the years, significant effort has been devoted in order to derive appropriate models of the structural behavior of rotating blades. It is beyond the scope of this paper to present a literature survey of this effort and only sources which are important to the presentation of this paper will be mentioned. The well known work of Houbolt and Brooks[1] was a stepping stone in the research of blade dynamics. In this outstanding research a consistent derivation of the structural model was presented, including solutions for special cases. The model of Ref. 1 has been used by many investigators in order to solve the complete aeroelastic behavior of blades. Moreover, many of the improved models which appeared since 1958, were in fact extensions of the structural model of Houbolt and Brooks.

Although the model of Ref. 1 includes nonlinear effects, the approach to nonlinear contributions is not accurate enough. The weakness of the model concerning the nonlinear effects is explained in detail in Ref. 2. Therefore, this model becomes insufficient when nonlinear effects become important.

During the years - as a result of introducing new designs, new manufacturing techniques and new materials - blades have become more flexible. Therefore the importance of nonlinear effects has grown to the point where consistent nonlinear structural models have become essential. As a result of this necessity, different nonlinear structural models of blades have been developed. Such a model is presented for example in Ref. 2 and compared with other models which exist in the literature. A survey of different models and the importance of nonlinear structural effects in the case of helicopter blades appear in Ref. 3. In order to obtain a consistent nonlinear model, most of the derivations include some kind of an ordering scheme[2,3]. According to this technique, each variable and unknown of the problem obtains an order of magnitude. This order of magnitude defines the limits of the model since when an ordering scheme demand ceases to exist, then the accuracy of the results is in question. Most of the nonlinear models, including the one which will be described in the present paper, are restricted to the case of small strains and moderate elastic rotations. Most of the engineering problems fall within the limits of these restrictions. The main advantage of using the ordering scheme is the fact that the decision what terms should be ignored becomes very clear. All the terms of certain order of magnitude and lower orders are retained in the equations while terms of higher orders are neglected.

The ordering scheme became a very powerful tool in obtaining consistent models. The very good agreement between the theoretical

predictions and experimental results, as presented for example in Ref. 4, is a proof of the capability of this technique. But on the other hand, the ordering-scheme technique has also certain weaknesses. It seems that one of the major problems is associated with the mathematical differentiation with respect to the spatial coordinate along the blade axis. In order to apply the technique, assumptions concerning the influence of differentiation on the ordering scheme should be adopted. Such assumptions are described in detail in Refs. 2,4 where it has been assumed that differentiation with respect to the nondimensional spanwise coordinate does not cause any change of the order or magnitude. Although such assumptions are very good in certain cases, they may cause increasing errors in others. In the model which will be described in the present paper the use of such assumptions, concerning the spatial differentiation, is avoided.

While a few years ago most of the blades had a straight (or almost straight) elastic axis, this is not the situation nowadays. The new generation of propellers, the prop-fans[5], have thin blades with curved elastic axis. Modern helicopter blades have swept tips and there are other rotating blades which have curved axis.

Most of the available structural models in the past were confined to the case of a straight elastic axis. Reference 6 presents a relatively early effort to deal with blades having an elastic axis which is not straight. But the structural model of[6] is over simplified and does not include different effects that may be important in the case of curved blades. It is interesting to note that during the last years different structural models for special kinds of curved rotating blades have been derived. These are the curved blades of Darrieus Wind Turbines. References 7 and 8 present such models and in[8] the results of the theoretical model exhibit very good agreement with experimental results of small models.

The purpose of the present paper is to present a nonlinear structural model of rotating blades. This model can also deal with blades having curved elastic axis. The model is very general and it can deal with any distribution of structural properties and loads along the blade. In addition, special effort is devoted to describe different combinations of boundary conditions which may exist in different practical applications. The analytical model is solved by using Galerkin method. In order to present the capabilities of the present model a few numerical examples will be presented and discussed.

The paper presents the results of a long lasting research during the last few years. The results of the different stages of this research are summarized in different reports and papers and it is not possible to present all these details in the present paper. Therefore, only a general view of the model and its capabilities will be presented here. The interested reader may find more details in papers and reports that will be mentioned in the text.

II. Description of the Structural Model

Geometrical Description

As already mentioned above, the derivation deals with blades which, from a structural point of view, can be looked upon as slender rods. In the case of slender rods a significant simplification of the problem is obtained by applying the Bernoulli-Euler hypothesis. As a result of this hypothesis the three-dimensional problem becomes a one-dimensional one. It is possible now to describe the deformation of each material point of the rod as a function of the deformations of the elastic axis. Therefore the blade is represented by its elastic axis.

The elastic axis of the blade is shown in Fig. 1. x_B, y_B and z_B represent a cartesian

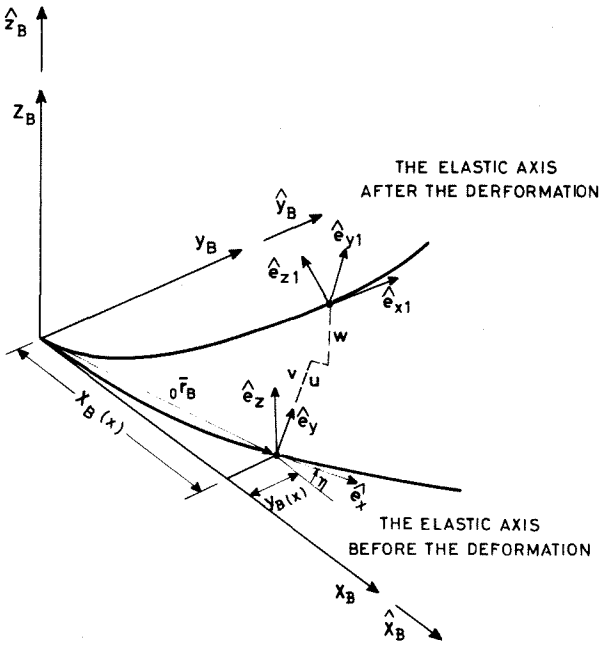

Fig. 1. The Elastic Axis of the Blade Before and after Deformation.

system of coordinates which is used to describe the elastic axis before the deformation. $\hat{x}_B$, $\hat{y}_B$ and $\hat{z}_B$ are unit vectors in the directions of the coordinate lines x_B, y_B and z_B, respectively. The derivation is restricted to the case of planar curved rods, since this is the situation in most of the practical cases and since the planar case presents a significant simplication in the equations. If necessary, the model can easily be extended to include also cases of three dimensional curvature. x is a curved coordinate line along the elastic axis. The geometry of the undeformed elastic axis is defined by the functions $x_B(x)$ and $y_B(x)$. The point x=0 is the blade root which is positioned at the origin of the system of coordinates ($x_B=y_B=z_B=0$). The length of blade is L and so the other tip is positioned at $x_B(L)$ and $y_B(L)$.

At each point along the elastic axis a triad of unit vectors $\hat{e}_x$, $\hat{e}_y$ and $\hat{e}_z$ is defined. $\hat{e}_x$ is tangent to the elastic axis, $\hat{e}_y$ is perpendicular to $\hat{e}_x$ and lies in the x_B-y_B plane, $\hat{e}_z$ is normal to this plane.

The blade is acted upon by distributed force $\bar{p}$ and moment $\bar{q}$, per unit length of the blade. As a result of these loads the blade deforms. The deformation of each point of the elastic axis is described by the displacement components u,v,w in the directions $\hat{e}_x$, $\hat{e}_y$, $\hat{e}_z$, respectively. In addition there is also a rotation ϕ about the elastic axis. As a result of this deformation the triad $\hat{e}_x$, $\hat{e}_y$, $\hat{e}_z$ is transformed into a new orthogonal triad of unit vectors: $\hat{e}_{x1}$, $\hat{e}_{y1}$, $\hat{e}_{z1}$, respectively (see Fig. 1). The loading vectors $\bar{p}$ and $\bar{q}$ are described by their components as follows:

$$\bar{p} = p_x\hat{e}_{x1} + p_y\hat{e}_{y1} + p_z\hat{e}_{z1} \tag{1a}$$

$$\bar{q} = q_x\hat{e}_{x1} + q_y\hat{e}_{y1} + q_z\hat{e}_{z1} \tag{1b}$$

The Equations of Equilibrium

In the derivation of the equations of equilibrium a few assumptions are adopted. These assumptions are outlined below:

a) As already mentioned above, the well known Bernoulli-Euler hypothesis is assumed to apply. According to this hypothesis plane cross-sections of the blade which are normal to the elastic axis before the deformation remain plane after deformation (except for very small deviations due to warping) and normal to the deformed elastic axis. In addition strains within the cross-sections are neglected.

b) The derivation is restricted to the case of small strains and moderate elastic rotations. According to this assumption strains and products of the elastic rotations are negligible compared to unity.

c) It is assumed that the warping displacements are small such that these displacements are negligible compared to typical cross-sectional dimensions.

d) y and z are cross-sectional coordinates in the directions $\hat{e}_{y1}$ and $\hat{e}_{z1}$ repectively. It is assumed that for any cross-sectional point $y\chi_y$ is negligible compared to unity. χ_y is the curvature of the undeformed elastic axis. y is a cross sectional coordinate in the e_{y1} direction. In cases when this assumption does not hold then Bernoulli-Euler hypothesis becomes questionable too.

These four assumptions are used throughout the derivation. At first, expressions for the strains are obtained and then, using the well known relations between stresses and strains in the case of slender rods, expressions for the stress components are obtained. Integration of the stress components over the blade cross-section yields the resultant cross-sectional force $\bar{F}$ and resultant cross-sectional moment $\bar{M}$. These resultants are described by their components as follows:

$$\bar{F} = P\hat{e}_{x1} + V_y\hat{e}_{y1} + V_z\hat{e}_{z1} \tag{2a}$$

$$\bar{M} = M_x\hat{e}_{x1} + M_y\hat{e}_{y1} + M_z\hat{e}_{z1} \tag{2b}$$

P is the axial force, V_y and V_z are the shearing force components, M_x the torsional moment, while M_y and M_z are the bending moment components. More details about all the above mentioned stages may be found in Refs. 9 and 10.

Now the equilibrium equations (forces and moments) for a small element of the deformed blade are derived. These equations contain the components of the cross-sectional resultant forces and moments, the curvatures and twist after the deformation, and the components of the applied loads. By eliminating the shearing force components, four equations of equilibrium are obtained. The four unknowns are u, v, w and ϕ, but as is common in different rod analyses, u is replaced as unknown by P. The detailed equations are given in Ref. 9.

Boundary Conditions

There are six boundary conditions at each boundary point of the blade. The homogeneous set of nonlinear boundary conditions is given by the following equation:

$$P + K_yM_z - K_zM_y = 0 \qquad \text{or } u = 0 \tag{3a}$$

$$V_y - TM_y = -M_{z,x} - K_zM_x - 2TM_y - q_z = 0 \qquad \text{or } v = 0 \tag{3b}$$

$$V_z - TM_z = M_{y,x} + K_yM_x - 2TM_z - q_y = 0 \qquad \text{or } w = 0 \tag{3c}$$

$$M_x = 0 \qquad \text{or } \phi = 0 \tag{3d}$$

$$M_z = 0 \qquad \text{or } v_{,x} = 0 \tag{3e}$$

$$M_y = 0 \qquad \text{or } w_{,x} = 0 \tag{3f}$$

K_y, K_z and T are the curvatures and twist at the boundary point. The conditions on the right side of Eqs. (3a-f) are the geometric conditons while those on the left side are conditions concerning forces and moments.

In most of the aeronautical applications of blades there is one edge where the resultant force and moment are zero and this edge is denoted the blade (free) tip (x=L). The blade is attached to the hub at the other edge which is denoted the blade root (x=0). But there are also special cases of different boundary conditions like for example the blades of the

Darrieus wind turbines[7,8].

Equations (3a-f) present most of the combinations of boundary conditions of rods which can be found in the literature. But in many practical cases of blades, the boundary conditions at the root are more complicated. In these cases the blade is not clamped to the hub, but instead there is an elastic rotational restraint there. This condition can be modeled as a certain moment at the blade root (and not zero as in Eqs. (3d-f)). The magnitude of this moment is determined by the loads' distribution along the blade. In many cases the loads along the blade are very sensitive to the rotations at the blade root. Such cases are solved by a careful coupling between the solution of the equilibrium equations and the conditions at the blade root.

Further discussion of the problem of boundary conditions appears in the next sections.

Calculating the Resultant Forces and Moments

The resultant forces and moments along the blade are calculated by two methods. In the first method, the expressions for the resultant forces and moments which are obtained during the derivation of the equations of equilibrium, are used. The expressions contain derivatives of the unknowns. It is well known that differentiation of the approximate expressions of the unknowns may increase the errors associated with the resultant forces and moments.

The second method is based on integration of the loads along the blade. The integration starts from the free tip and ends at any cross-section of the blade where the resultant force and moment are calculated. The integration includes all the nolinear effects. Since this method does not include differentiation it is expected to yield more accurate results compared to the first method.

III. Method of Solution

The system of equilibrium equations is solved by using Galerkin method. According to this method the unknowns (nondimensionalized for convenience) are described by the following series:

$$\overset{\circ}{v} = v/L = \sum_{j=1}^{N_v} v_j FV_j \qquad (4a)$$

$$\overset{\circ}{w} = w/L = \sum_{k=1}^{N_w} w_k FW_k \qquad (4b)$$

$$\phi = \sum_{l=1}^{N_\phi} \phi_l F\phi_l \qquad (4c)$$

$$\overset{\circ}{P} = PL^2/Eb^4 = \sum_{m=1}^{N_p} p_m FP_m \qquad (4d)$$

FV_j, FW_k, $F\phi_l$ and FP_m are pre-determined shape functions that satisfy the boundary conditions that must be satisfied by $\overset{\circ}{v}$, w, ϕ and $\overset{\circ}{P}$, respectively. E is a representative modulus of elasticity while b is a typical cross-sectional dimension. The unknowns become the coefficients v_j, w_k, ϕ_l and p_m. The numbers of these unknowns are N_v, N_w, N_ϕ and N_p, respectively. In cases where an elastic restraint exists at the blade root, special approach is needed. After a few trials it was found that an efficient method to cope with this problem is when a limited number of terms in the series takes care of the inhomogeneous boundary conditions while the other terms satisfy an homogeneous set of boundary conditions. An example of using this approach is presented in the next section.

IV. Results and Discussion

The purpose of this section is to present the capability of the model which has been described in the previous sections. Two examples will be presented. The first example deals with a blade which is clamped at its root and free at its other boundary point. This blade does not rotate and is loaded by a uniform distributed static load. The second example presents the case of a rotating blade where distributed inertial and aerodynamic loads are acting along it. Since the main purpose of the paper is to present the structural model, only a very simple aerodynamic model will be used.

Example No. 1

The elastic axis of the blade is shown in Fig. 2. This is a swept back blade and therefore

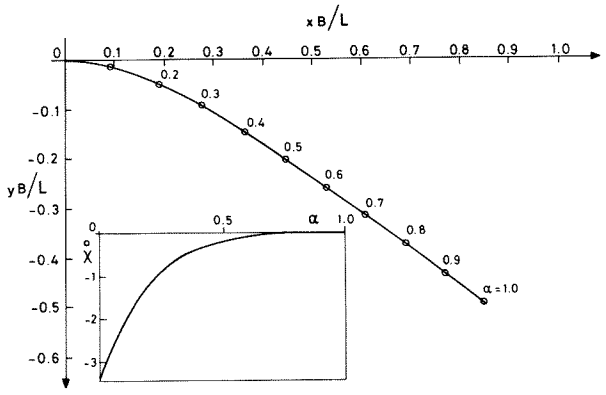

Fig. 2. The Elastic Axis of the Blade and its Curvature (Examples 1,2).

negative values of y_B are used. The blade is swept by an angle of 36° at its tip (there is a zero sweep angle at the root). Figure 2 also presents the nondimensionalized curvature along the blade. The structural properties are uniform along the blade and are equal to:

$$EI_{yy}/Eb^4=0.0417,\ EI_{zz}/Eb^4=0.0104,$$

$$GJ/Eb^4=0.011,\ EI_{yz}=0 \qquad (5)$$

EI_{yy} is the edgewise components of the bending stiffness (in the x_B-y_B plane), EI_{zz} is the beamwise component (out of plane) and GJ the torsional stiffness. It is assumed that the tension center of the blade coincides with its shear center.

The blade is acted upon by a uniform distributed force of "gravity type" (this means that the force inertial-direction and magnitude are not changed as a result of the blade deformation). The distributed force acts in a plane which is parallel to the y_B-z_B plane. The angle between the load and the x_B-y_B plane is 45°. The magnitude of the load (per unit length of the blade) is p_g while the non-dimensional value is denoted $\overset{\circ}{p}_g$ and is defined as follows: $\overset{\circ}{p}_g=p_g L^3/Eb^4$.

The blade is clamped at the root and free at the tip. Based on these boundary conditions the shape functions of Eqs. (4a-d) have been chosen. FV_j and FW_k are identical and are the natural modes of vibration of a clamped/free uniform straight beam[11,12]. $F\phi_l$ are the torsional modes of vibration of a fixed/free uniform straight beam. FP_m are given by:

$$FP_1 = 1 - \alpha^2$$

$$FP_m = \sin[\pi(m-1.5)(1-x/L)] \qquad m \geq 2 \qquad (6)$$

All the shape functions are normalized such that their maximum value is unity. N_V and N_W (see Eqs. 4a-d) have been chosen equal to three while N_ϕ and N_P are equal to five. The convergence of the coefficients of the series which describe the unknowns is presented in the next Table. All the coefficients have been normalized with respect to the first coefficient in each series. The load is equal to $\overset{\circ}{p}_g=0.0274$ and all the results of this example will refer to this load.

i	v_i/v_1	w_i/w_1	ϕ_i/ϕ_1	p_i/p_1
1	1	1	1	1
2	0.0132	0.0166	-0.0574	-1.036
3	0.000168	0.00113	-0.142	-0.0386
4			-0.0899	-0.00616
5			-0.0564	-0.00370

Table 1. The Coefficients of Example 1 (initial choice of shape functions).

It can be seen that the convergence of the series which describe v and w is very good. v and w themselves are shown in Figs. 3, 4, respectively.

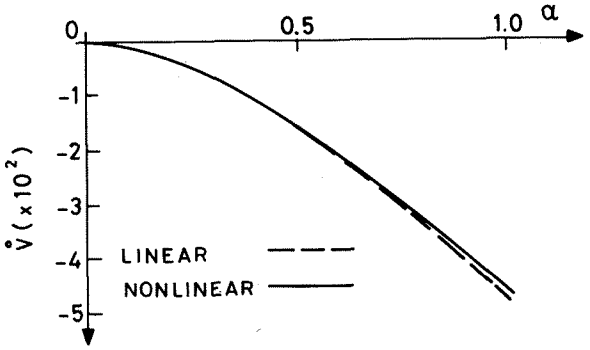

Fig. 3. The Spanwise Distribution of the Non-Dimensional Edgewise Displacement Component (Example 1).

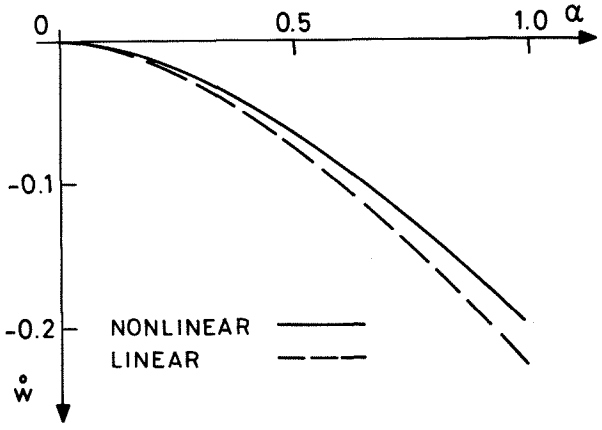

Fig. 4. The Spanwise Distribution of the Non-Dimensional Beamwise Displacement Component (Example 1).

As expected from Table 1 these transverse displacement components are dominated by the first mode. In Figs. 3,4 the nonlinear results are also compared with the results of a linear model where all the nonlinear effects are neglected. While the influence of nonlinear effects on v is small, there are changes of up to 16% in $\overset{\circ}{w}$ due to the influence of nonlinear effects.

The convergence of the series which describes the elastic angle of rotation about the elastic axis, $\overset{\circ}{\phi}$, is not as good as in the series of v and w. Although the first term in the series is greater by an order of magnitude compared to all the others, the convergence among the other terms is poor. The difficulty is understood if one examines $\overset{\circ}{\phi}$ as described by Fig. 5 (the broken line). At the blade root region this angle is positive and is the result of the torsional moment component, M_x. At the outer portion of the blade, this angle is negative and is mainly the

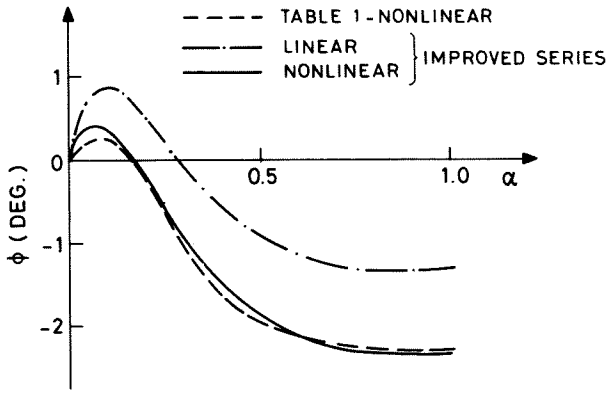

Fig. 5. The Spanwise Distribution of the Angle of Rotation about the Elastic Axis (Example 1).

result of the transverse displacement of the curved blade. It is very difficult for the shape functions which have been chosen to describe the relatively drastic change of behavior at the root, and this is the reason for the convergence problems. This problem will become more significant when the distribution of the torsional moment, M_x, will be discussed.

The distributions of the nondimensional bending moment components along the blade are shown in Figs. 6 and 7. (The nondimensional components

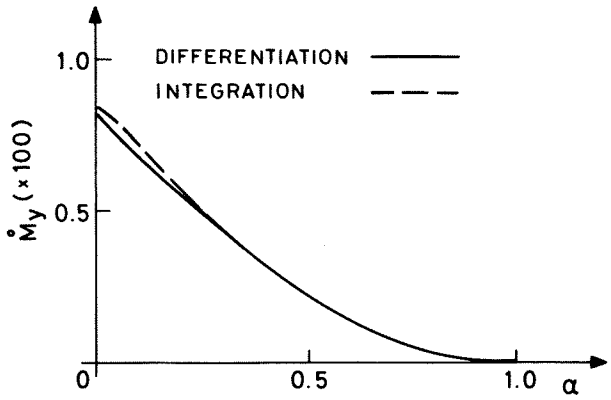

Fig. 6. The Spanwise Distribution of the Non-Dimensional Beamwise Bending Moment Component (Example 1).

$\mathring{M}_x, \mathring{M}_y, \mathring{M}_z$ are obtained after dividing the dimensional components by Eb^4/L). They exhibit the typical bending moment distribution of a cantilevered beam. In the figures the results of the two methods of calculating the resultant moment, differentiation vs. integration, are compared. As can be seen, the agreement between the two methods is very good.

In Fig. 8 the spanwise distribution of the

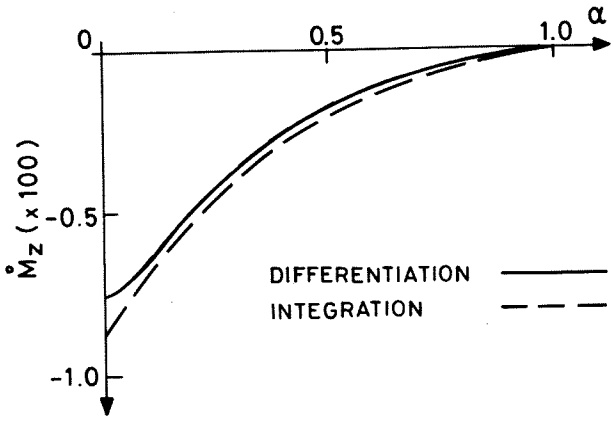

Fig. 7. The Spanwise Distribution of the Non-Dimensional Edgewise Bending Moment Component (Example 1).

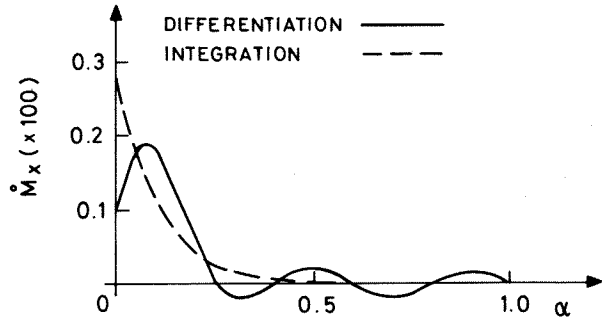

Fig. 8. The Spanwise Distribution of the Non-Dimensional Torsional Moment (According to the results of Table 1 - Example 1).

torsional moment M_x is presented. The problems which have been discussed previously concerning the angle ϕ, appear here in a more significant manner. It turns out that it is very difficult to describe the sharp change at the blade root by using the shape functions which have been chosen to describe ϕ. In order to overcome these problems another series for ϕ has been tried. In this series only the first three shape functions of the previous series are retained. The fourth and fifth shape functions are replaced by the functions which are shown in Fig. 9. These shape functions are described by the following equation:

$$F\phi_1 = A(B\alpha^4 + C\alpha^3 + D\alpha^2 + \alpha)e^{-k\alpha} \qquad (7)$$

$$B = D + 2 \; ; \; C = -(3+2D) \; ; \; D = \frac{8\alpha_m^2 - \alpha_m - 1}{2\alpha_m(1-2\alpha_m)}$$

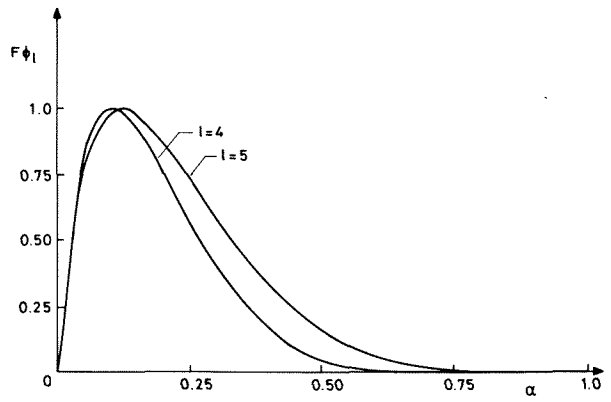

Fig. 9. The Fourth and Fifth Shape Functions of the Improved Series for ϕ (Example 1).

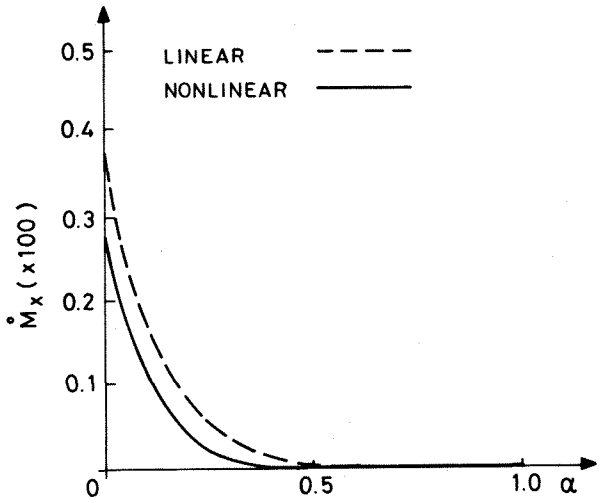

Fig. 10. The Spanwise Distribution of the Non-Dimensional Torsional Moment (According to the Improved series - Example 1).

For the fourth shape function: α_m=0.2; A=24.358, k=5. For the fifth shape function: α_m=0.3; A=20.582, k=5. These last two functions satisfy the necessary boundary conditions and in addition they are also zero at the free tip. Their influence is concentrated at the blade root and their purpose is to describe the sharp changes at the blade root, while having very small influence at the outer region of the blade. By choosing appropriate values of α_m, A and k, shape functions which are appropriate for different distributions of curvature may be obtained. Using the improved series, the column for ϕ_i/ϕ_1 in Table 1 is replaced by the following vector: 1, 0.102, -0.00203, -0.0745, -0.288. It can be seen that the convergence of the three first coefficients is very good. The last two coefficients help to improve the results at the root region. The spanwise distribution of ϕ for the improved series is shown in Fig. 5. The results of the nonlinear case are compared with the results of a linear model. It can be seen that ϕ presents the largest differences between the linear and nonlinear model. It also can be seen that the differences, between the results of the improved series (for ϕ) and the previous series, are concentrated near the blade root. A significant improvement in predicting M_x is obtained by using the improved series for ϕ. As can be seen from Fig. 10 the agreement between the results of the differentiation and integration methods is excellent and they practically coincide. The results of the differentiation method while using the linear model are also presented. There are deviations of up to 70% between the linear and nonlinear results.

In Table 1 the results of the axial component of the cross-sectional resultant force are also presented. But since this component is very small and unimportant in the present example, further discussion is not presented.

Example No. 2

This example deals with a hovering rotor. The rotor has four identical, equally spaced, curved blades and it rotates with a constant angular velocity Ω=150 rad/sec. The geometry of the elastic axis of the blades is identical to the geometry of the blade of the previous example (see Fig. 2) and its length 1.5 m. All the blades are connected to the shaft with a zero offset. The boundary conditions at the blade root are such that the blade is clamped with respect to the edgewise displacement v, and the angle ϕ is also zero at the root. There is a flapping hinge at the root (the direction of this hinge coincides with y_B). The blade rotation about this hinge is restrained by a linear torsional spring the stiffness of which is 28470 N.m/rad. This spring exerts zero moment when the blade lies at x_B-y_B plane.

The blade has a uniform distribution of the structural, inertial and aerodynamic properties. The structural properties are equal to:

$$EI_{yy}=0.8859\times10^{6}\ N\ m^2\ ;\quad EI_{zz}=0.8859\times10^{4}\ N\ m^2;$$

$$EI_{yz}=0\ ;\ GJ=0.9\times10^{4}\ N\ m^2 \qquad (8)$$

The tension center of each cross-section coincides with the cross-sectional shear center, mass center and aerodynamic center.

The mass per unit length of the blade equals 2.25 kg/m. The cross-sectional components of the mass moment of inertia are:

$$MI_{yy}=0.4219\ 10^{-3}kg\ m;\ MI_{zz}=0.4219\ 10^{-5}kg\ m;\ MI_{yz}=0 \qquad (9)$$

The aerodynamic chord equals 0.15 m while the pitch angle of each cross-section (relative to the x_B-y_B plane) equals 8°. As indicated before a simple aerodynamic model of the loads along the blades has been chosen. A uniform inflow velocity is assumed which is equal to 9 m/sec. The lift and drag at each cross-section are calculated by applying two dimensional properties of the airfoil

(tip effects are neglected). The drag coefficient is given by

$$C_D = 0.01 + 0.015\, C_L^2 \qquad (10)$$

The air mass density in all the calculations is equal to 1.23 kg/m^3. Since the blade rotates about the flapping hinge, there is a rigid body rotation degree of freedom in addition to the elastic deformations. This rotation is denoted by β. The shape functions for v are identical to those of the previous example (N_v=3). The series for w also includes three terms. The first shape function in this series is the first mode of vibration of a clamped/free uniform beam. The coefficient of this term is determined according to the magnitude of the flapping moment at the blade root. The second and third shape functions in the series which describes w are the first and second modes of vibration of a simply-supported/free uniform beam. The shape functions $F\phi_1$ and $F\phi_2$ are identical to those of the first example. $F\phi_3$ of the present example is identical to $F\phi_4$ of the previous one. The series for P is identical for the two examples.

The hovering case presents a "steady state" of equilibrium. Because of the highly nonlinear nature of this phenomenon, its very difficult to obtain this steady-state by direct static solution (the solution procedure tends to diverge). It has been found that the easiest way of obtaining this solution is by starting from some initial condition and applying an integration with respect to time until the steady state is obtained[9]. When the natural physical damping forces and moments are added to the model it is quite easy (although time consuming) to obtain the solution. In Fig. 11 the behavior of the coefficients along the first revolution of the rotor is presented. All the initial conditions (states and velocities) are taken equal to zero. In Fig. 11 also the final steady state values of the coefficients of the series are presented.

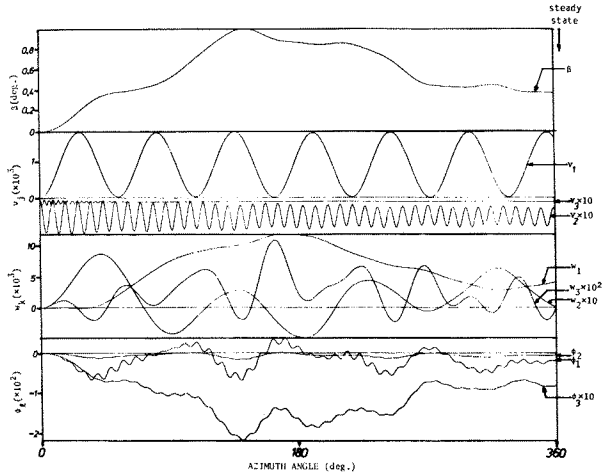

Fig. 11. The Behavior of the Coefficients along the First Revolution and the Steady State Values (Example 2).

In Fig. 12 the nondimensional displacement component $\mathring{v}$ along the blade is presented. This displacement is mainly the result of the high centrifugal forces which tend to straighten the blade. $\mathring{w}$ is presented in Fig. 13. In addition to the displacement w there is also a rigid body rotation of 0.58° about the flapping hinge. As a result of the presence of the elastic restraint at the root, this rotation together with the elastic angles of rotation about the flapping hinge (as presented by the second and third terms in the series for w), determine the flapping moment at

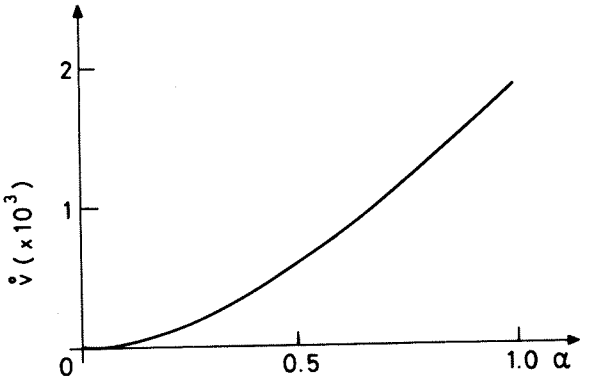

Fig. 12. The Spanwise Distribution of the Non-Dimensional Edgewise Displacement Component (Example 2).

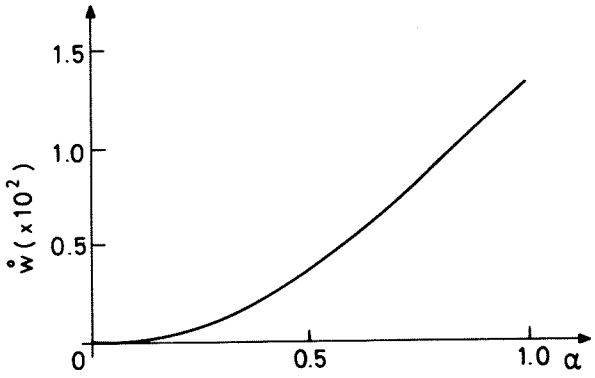

Fig. 13. The Spanwise Distribution of the Non-Dimensional Beamwise Displacement Component (Example 2).

the blade root. This flapping moment determines the coefficient w_1 in the series for w.

The elastic rotation ϕ is shown in Fig. 14.

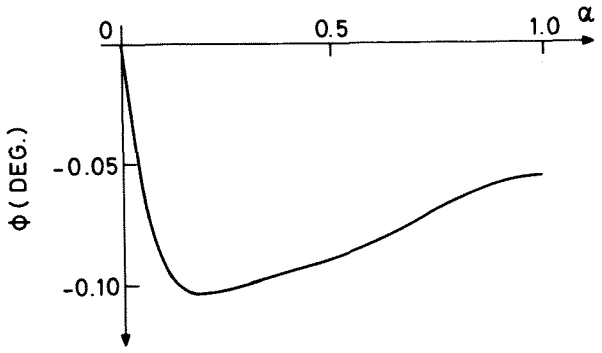

Fig. 14. The Spanwise Distribution of the Angle of Rotation About the Elastic Axis (Example 2).

The trends in the behavior of ϕ are similar to what has been discussed in the first example. The large negative torsional moment at the root region cause a steep increase in the negative elastic angles of rotation. At the outer region the magnitude of this negative rotation is decreased as a result of the increased transverse displacement which tend to contribute positive values of ϕ. The distribution of the nondimensional axial component of the resultant force along the blade is presented in Fig. 15. The results of the series are compared to the results of integration of the loads along the blade. The agreement between the two methods is good.

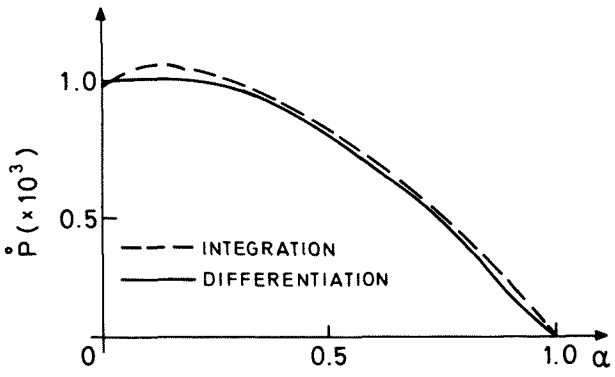

Fig. 15. The Spanwise Distribution of the Non-Dimensional Axial Component of the Resultant Force (Example 2).

The distribution of the resultant moment components is shown in Figs. 16-18. As in the

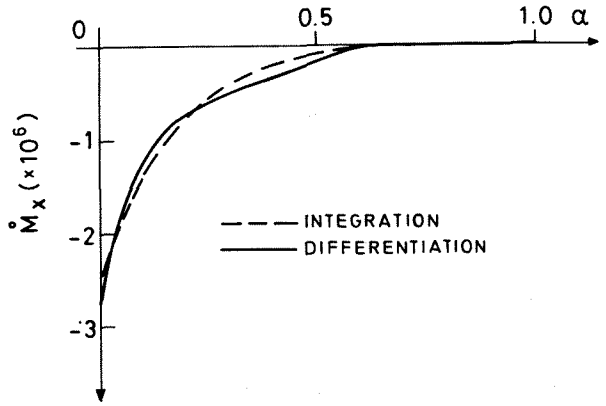

Fig. 16. The Spanwise Distribution of the Non-Dimensional Torsional Moment (Example 2).

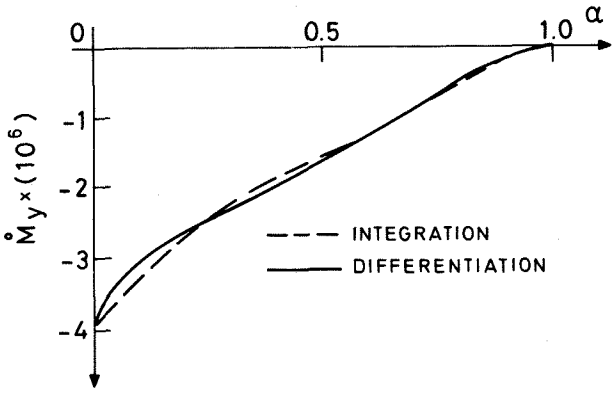

Fig. 17. The Spanwise Distribution of the Non-Dimensional Beamwise Bending Moment Component (Example 2).

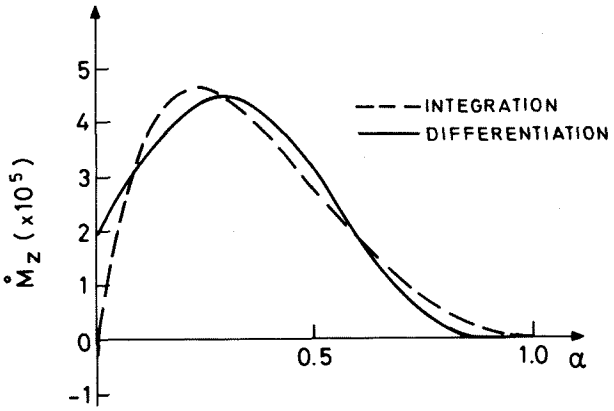

Fig. 18. The Spanwise Distribution of the Non-Dimensional Edgewise Bending Moment Component (Example 2).

first example, there is a relatively shape increase in $\mathring{M}_x$ near the blade root, due to the large curvature in this region. The agreement between the differentiation and integration methods is

good. Good agreement is also obtained in the case of M_y. M_z exhibits an interesting behavior. Being mainly the result of the centrifugal contributions, this moment tends to disappear at the blade root (the moment due to inertial contributions becomes zero while only aerodynamic contributions are left). While the integration results are probably accurate, the differentiation results exhibit increasing deviations in certain cross-sections although the nature of the behavior is identical in both methods. Increasing the number of terms in the series for v will probably improve the agreement.

V. Conclusions

A general nonlinear model of the structural behavior of rotating blades has been presented. The model includes curved blades having any distribution of planar curvature. Any distribution of structural properties along the blade can be dealt with. In addition, to the classical nonlinear combinations of boundary conditions, it is also possible to analyse cases of root hinges and elastic restraints at the blade root.

Galerkin method is used in order to solve the equilibrium equations. Special treatment is needed in order to deal with the different kinds of boundary conditions. By using Galerkin method an efficient numerical scheme is obtained.

The resultant moment distribution along the blade is calculated by two methods: the first method is based on the structural expressions and includes differentiation of the elastic displacements along the blade, the second method includes integration of the loads along the blade. Both methods include nonlinear effects.

Two numerical examples have been presented. It has been shown that the behavior of curved blades is much more complicated than straight blades. Comparison between the two methods of calculating the resultant moment distribution shows good agreement in most of the cases. This good agreement is obtained only if appropriate shape function in the Galerkin series are used.

It seems that curved blades may have many beneficial effects from: aeroelastic, aerodynamic and acoustic points of view. But special care must be devoted in order to take all the aspects of curvature into account.

Acknowledgement

The authors would like to thank Mrs. A. Goodman-Pinto for typing the paper and Mrs. E. Nitzan and R. Puvlic for the preparation of the figures.

List of References

1. J.C. Houbolt and G.W. Brooks, "Differential Equations of Motion for Combined Flapwise Bending, Chordwise Bending, and Torsion of Twisted Nonuniform Rotor Blades", NACA Report 1346, 1958.

2. A. Rosen and P. Friedmann, "Nonlinear Equations of Equilibrium for Elastic Helicopter or Wing Turbine Blades Undergoing Moderate Deformation", UCLA-ENG-7718, Revised Edition, June 1977.

3. P. Friedmann, "Formulation and Solution of Rotary Wing Aeroelastic Stability and Response Problems", Vertica, Vol. 7, No. 2, 1983, pp. 101-142.

4. A. Rosen and P. Friedmann, "The Nonlinear Behavior of Elastic Slender Straight Beams Undergoing Small Strains and Moderate Rotations", Proceedings of ASME, J. of Applied Mechanics, Vol. 46, 1979, pp. 161-168.

5. J.F. Dugan, B.D. Gatzen and W.M. Adamson, "Prop-Fan Propulsion - Its Status and Potential", SAE 780995, Aerospace Meeting, November 27-30, 1979.

6. J.R. Van Gaasbeek, T.T. Mclarty and S.G. Sadler, "Rotorcraft Flight Simulation, Computer Program C81, Vol. I - Engineer's Manual", Bell Helicopter Texteron, USARTL-TR-77-54A, October 1979.

7. K.R.V. Kaza and R.G. Kvaternik, "Aeroelastic Equations of Motion of A Darrieus VAWT Blade", NASA TM-79295, Dec. 1979.

8. A. Rosen and H. Abramovich, "Investigation of the Structural Behaviour of the Blades of a Darrieus Wind Turbine", Proceedings of the 4th International Symposium on Wind Energy Systems, Stockholm, Sweden, September 21-24, 1982, paper H3, Vol. 2, pp. 39-58.

9. A. Rosen and O. Rand, "A General Model of the Dynamics of Moving and Rotating Curved Rods", Department of Aeronautical Engineering, Technion, TAE No. 514, September 1983, 102 pp.

10. A. Rosen and O. Rand, "Formulation of a Nonlinear Model for Curved Rods", Proceedings of the 26th Israel Annual Conference on Aviation and Astronautics, Israel, February 8-9, 1984, pp. 244-256.

11. D. Young and R.P. Felgar, "Tables of the Characteristic Functions Representing Normal Modes of Vibration of a Beam", The University of Texas Publication No. 4913, July 1949.

12. E. Volterra and E.C. Zachmanoglou, "Dynamics of Vibrations", Charles E. Merrill Books, Inc., 1965, pp. 319-320.